TM-70-2013-1

TECHNICAL MEMORANDUM

Bellcomm

FACILITY FORM 602
(PAGES)
(CODE)
NASA CR OR TMX OR AD NUMBER
(CATEGORY)

BELLCOMM, INC.
955 L'ENFANT PLAZA NORTH, S.W., WASHINGTON, D.C. 20024

COVER SHEET FOR TECHNICAL MEMORANDUM

TITLE- Parametric Analysis of Three-Impulse Transfer Between Hyperbolic Lunar Orbit and a Circular Lunar Parking Orbit

TM- 70-2013-1

DATE- March 18, 1970

FILING CASE NO(S)- 310

AUTHOR(S)- M. R. Kerr

FILING SUBJECT(S)-
(ASSIGNED BY AUTHOR(S))- Three-Impulse Transfer,
Trajectory Optimization,
Hyperbola to Circular Orbit Transfer

ABSTRACT

Optimized three-impulse transfers from a hyperbolic lunar trajectory to a circular parking orbit have been analyzed parametrically. From the data presented, both the three-impulse and one-impulse ΔV costs can be determined given a vector velocity at the lunar sphere of influence and a lunar parking orbit unit angular momentum vector.

The ΔV savings of the three-impulse technique over the one-impulse can be as high as 4600 fps. For a landing site far off the lunar equator such as Tycho, the LOI ΔV cost is typically reduced from 5000 fps to 3000 fps.

BA-145A (8-68)

SEE REVERSE SIDE FOR DISTRIBUTION LIST

DISTRIBUTION

COMPLETE MEMORANDUM TO

CORRESPONDENCE FILES:

OFFICIAL FILE COPY
plus one white copy for each additional case referenced

TECHNICAL LIBRARY (4)

NASA Headquarters

T. A. Keegan/MA
W. E. Stoney/MA

NASA MSC

R. L. Berry/FM5
J. R. Elk/FM5
C. Huss/FM
C. A. Perrine/PD
G. A. Weisskopf/FM5

Bellcomm, Inc.

D. R. Anselmo
A. P. Boysen, Jr.
J. O. Cappellari, Jr.
D. A. DeGraaf
D. R. Hagner
W. G. Heffron
B. T. Howard
D. B. James
S. L. Levie
P. F. Long
J. L. Marshall, Jr.
K. E. Martersteck
J. Z. Menard
P. E. Reynolds
J. W. Timko
R. L. Wagner
M. P. Wilson
All Members Department 2013

COVER SHEET ONLY TO

NASA Headquarters

R. A. Petrone/MA

Bellcomm, Inc.

I. M. Ross

BA-146 (8-64)

BELLCOMM, INC.
955 L'ENFANT PLAZA NORTH, S.W. WASHINGTON, D. C. 20024

SUBJECT: Parametric Analysis of Three-Impulse Transfer Between a Hyperbolic Lunar Orbit and a Circular Lunar Parking Orbit Case 310

DATE: March 18, 1970

FROM: M. R. Kerr

TM-70-2013-1

TECHNICAL MEMORANDUM

INTRODUCTION

The purpose of this paper is to examine parametrically both one- and three-impulse ΔV costs into (or out of) a circular lunar parking orbit under different boundary conditions and to determine under what conditions a three-impulse maneuver should be employed.

The three-impulse transfer considered in this study consists of the following maneuvers: 1) transfer from the hyperbola to a first ellipse, 2) transfer from the first ellipse to a second ellipse, 3) transfer from the second ellipse to a final circular parking orbit. The second and third maneuvers involve both an energy change and a plane change while the first maneuver is constrained to occur in the plane of the hyperbola.

The boundary conditions for the transfer geometry from the hyperbola to the circular parking orbit are established by specifying the vector velocity relative to the moon at the moon's sphere of influence, $\vec{V}_\infty$, and the unit angular momentum vector of the desired final parking orbit. In this study the circular parking orbit is taken as the reference plane. All conics were generated subject to the constraint that perilune altitude be greater than 40 nm. The approach hyperbola for the three-impulse maneuvers was targeted to a perilune altitude of 150 nm. The final circular parking orbit altitude was 60 nm.

The discussion that follows is in terms of lunar orbit insertion, LOI, that is transfer from a hyperbolic orbit into a parking orbit. The results are equally applicable to transearth injection.

THREE-IMPULSE METHOD

If an initial hyperbola and a final parking orbit are assumed, there are eight parameters necessary to specify the three-impulse geometry completely:

1. Apolune radius of the first ellipse, r_a.
2. True anomaly on the hyperbola at the first burn, f_{1A}.
3. True anomaly on the first ellipse at the first burn, f_{1B}.
4. Plane change at the first burn, ρ_1.
5. True anomaly on the first ellipse at the second burn, f_{2A}.
6. True anomaly on the second ellipse at the second burn, f_{2B}.
7. Plane change at the second burn, ρ_2.
8. True anomaly on the second ellipse at the third burn, f_{3A}.

See Figures 1, 2, 3 and 4 for the actual geometry. The version of the three-impulse optimization used in this study consists of a three-dimensional linear search[1] on f_{1A}, f_{1B} and f_{2A}. The transfer from the hyperbola to the first ellipse is constrained to be coplanar, that is $\rho_1 = 0$ since it was found that optimizing ρ_1 yields a negligible ΔV advantage. This is not surprising since the basic advantage of the three-impulse maneuver is derived from performing the required plane change at the second burn, near apolune of the intermediate ellipse, where the velocity is low. These parameters specify the first burn completely and determine the position and velocity prior to the second burn.

The optimum transfer trajectory from the state at the initiation of the second burn to the final burn is obtained by using a method developed by Fang Toh Sun[2,3]. The final state is specified by the angle, Θ, from the projection of the

radius vector at the second burn on the circular orbit to the final radius vector. See Figure 5. A linear walk optimization is performed on θ, internal to the linear search on f_{1A}, f_{1B}, and f_{2A}.

APPROACH HYPERBOLA

The approach hyperbola is optimized external to the three-impulse optimization. Figure 6 graphically defines the parameters used to construct the approach hyperbola for the three-impulse trajectory. The final parking-orbit plane, defined by a unit angular momentum vector, $\vec{H}$, is the reference. ϕ defines the out-of-plane angle of $\vec{V}_\infty$.

The MSI pierce point remains to be defined to specify the hyperbola. If a perilune radius of the hyperbola is selected, there is a circular locus of possible pierce points on the MSI centered about the negative $\vec{V}_\infty$. The flight path azimuth at the MSI, α, (shown in Figure 6) defines a single member of the family of hyperbolas defined by the pierce point locus. Total LOI ΔV is minimized with respect to α.

It is necessary to constrain the minimum perilune altitude of each intermediate ellipse and the hyperbola. Within this constraint it is possible to optimize the hyperbola perilune. It was found that the optimum varied between 60 and 150 nm depending on the values of ϕ and V_∞ and that the maximum benefit for optimizing the hyperbola perilune was on the order of 30 fps. Therefore, to simplify the analysis, the hyperbola perilune altitude was arbitrarily constrained to 150 nm.

The optimum one-impulse hyperbola was found by a different method. $\vec{V}_\infty$ was defined as in the three-impulse construction. The constraint that perilune altitude of the hyperbola be greater than 40 nm was imposed. The optimum MSI pierce point was determined by minimizing the total angle between the required velocity for a circular orbit and the pre-maneuver velocity vector. The method used is discussed in Reference 4.

THREE-IMPULSE AND ONE-IMPULSE ΔV COST

The parameters used to specify the one-impulse LOI were V_∞ and ϕ. Values of V_∞ ranging from 2700 fps to 3600 fps were selected, which correspond to translunar flight times from 70 to 110 hours for mean earth-moon distance. ϕ was varied from 10 to 85 degrees. The three-impulse LOI was further specified by the apolune radius of the first ellipse, r_a. Values of r_a ranging from 1438.5 nm to 12000 nm were considered.

Figures 7, 8, 9 and 10 illustrate the LOI ΔV costs for the different cases. When ϕ is greater than a particular value, dependent on V_∞ and r_a, a three-impulse maneuver is cheaper than the one-burn maneuver, with the ΔV advantages ranging from 0 to 4600 fps depending on the initial energy and apolune of the first ellipse. Figure 11 graphically shows the ranges of ϕ in which a three-impulse trajectory will give a ΔV advantage over the one-impulse. The large advantage of the three-burn technique is the result of the relatively cheap plane change ΔV at the second burn. As apolune increases the cost of the second burn decreases.

As one would expect, the LOI ΔV cost increases for the three-impulse maneuver as V_∞ increases since the first burn becomes more expensive as the energy difference increases. For a given apolune the increase in LOI ΔV at the first burn is $\sim$ 100 fps per 300 fps increase in V_∞. There is no increase in the second or third burn due to the increase in V_∞.

The one-burn data behave differently. For ϕ greater than about 20 degrees, the one-burn ΔV decreases as V_∞ increases. This is the result of the optimum injection point occurring closer to the minimum possible plane change point, that is where the plane change equals ϕ. Hence, even though the required energy change is greater for larger V_∞, the lower required plane change results in a lower total ΔV.

For values of ϕ above about 50 degrees it is impossible to achieve a one-burn LOI within the perilune constraint. A three-impulse trajectory is possible for the entire range of ϕ considered.

Figures 12, 13, 14 show the individual maneuver costs for each of the three-impulse maneuvers with a V_∞ of 2700 fps. The first-burn cost, ΔV_1, increases as the apolune radius of the first ellipse decreases. This is due to the increasing energy difference between the hyperbola and the first ellipse. The second-burn cost, ΔV_2, also increases as the apolune radius of the first ellipse decreases. Since the burn occurs closer to the moon as r_a decreases, the velocity increment necessary to do a plane change to the second ellipse increases. The third-burn cost, ΔV_3, decreases as r_a decreases due to the smaller energy difference between the second ellipse and the final circular orbit.

The scatter of the data points about the plotted curves in Figures 12, 13 and 14 is due to noise in the optimization of f_{1A}, f_{1B} and f_{2A}. The large transient in the region of $\phi = 55°$ for the 12000 nm ellipse in Figures 12 and 13 is due to a shift in the optimum f_{1A} from $\sim 0°$ to $\sim 50°$ which results in compensating changes in ΔV_1 and ΔV_2 to produce a smooth total ΔV curve.

TIME OF FLIGHT BETWEEN THE FIRST AND THIRD BURNS

Time of flight between the first and third burns is a function of r_a and V_∞ as shown in Figure 15. As the inclination of the approach hyperbola increases the time of flight decreases. This is due to the fact that the first burn of the optimized three-impulse maneuver tends to occur at larger true anomalies at high inclinations, thus reducing the time in the first ellipse. Time of flight does not vary very much with inclination or V_∞ for the small first ellipses. The trajectories containing large intermediate ellipses have more variation in time of flight. The variation is a result of f_{1B} increasing as ϕ increases and f_{1B} decreasing as V_∞ increases. The time spent in the first ellipse is larger when f_{1B} is smaller.

SUMMARY

Three-impulse and one-impulse transfers between hyperbolic lunar trajectories and a circular lunar orbit have been examined for a range of hyperbola parameters (V_∞ and ϕ).

Three-impulse ΔV savings at LOI have been shown to range from zero up to 4600 fps.

By using Figure 12 it is possible to determine the conditions under which a three-impulse trajectory will give a ΔV advantage given the ϕ and V_∞ required. One convenient way to use this data is to first generate a trajectory using a one-burn LOI. The required V_∞ and ϕ or ΔV_{LOI} taken from that trajectory may then be used to determine if a three-burn advantage exists. The magnitude of the ΔV savings may be determined from Figures 7 through 10.

A mission to Tycho launched on February 6, 1973 has a V_∞ of 3340 fps and one-burn ΔV_{LOI} of 4256 fps. Referring to Figure 10, it is estimated that a three-impulse trajectory, with r_a = 10,000 nm launched on the same date, would result in a LOI ΔV of only 3200 fps.

M. R. Kerr

2013-MRK-slr

M. R. Kerr

Attachments

REFERENCES

1. Levie, S. L., Jr., "PATERN, A Direct Search Minimization Routine," Bellcomm Memorandum for File, June 20, 1968.

2. Sun, Fang Toh, "Analysis of the Optimum Two Impulse Orbital Transfer Under Arbitrary Conditions," AIAA Journal, Vol. 6, No. 11, November 1968, pp 2145-53.

3. R. A. Bass, E. A. McGinness, "A Method for Determining Minimum ΔV Two Impulse Transfer Trajectories between Arbitrary State Vectors and Its Application to Three Impulse LOI Optimization," Bellcomm Memorandum for File, September 24, 1969.

4. Amman, R. J., "Mission Analysis and Open-Loop Trajectory Targeting Theory for the Bellcomm Apollo Simulation Program," Bell Telephone Laboratories Technical Memorandum, MM66-4264-2, January 10, 1966.

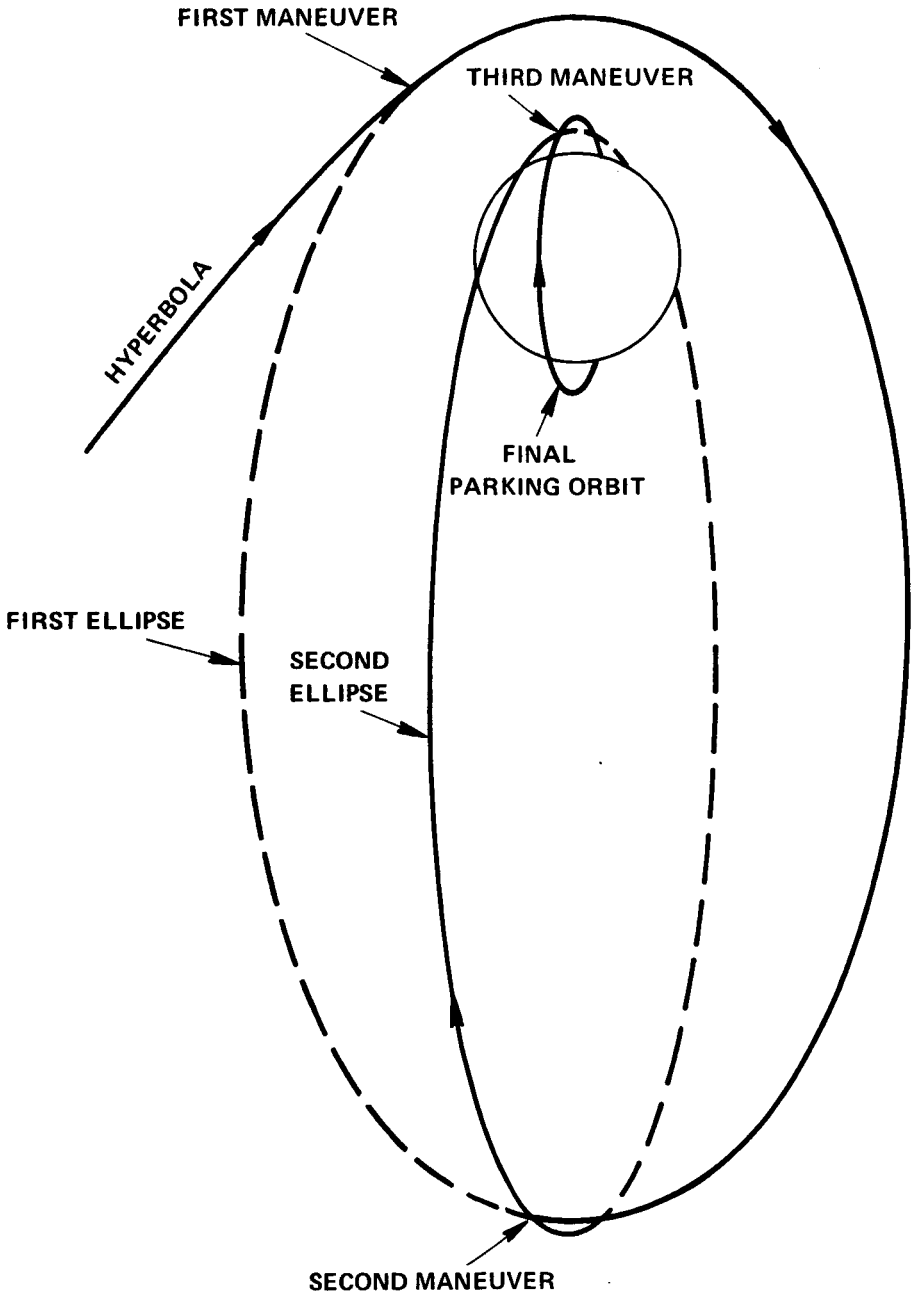

FIGURE 1 - GENERAL THREE-IMPULSE GEOMETRY

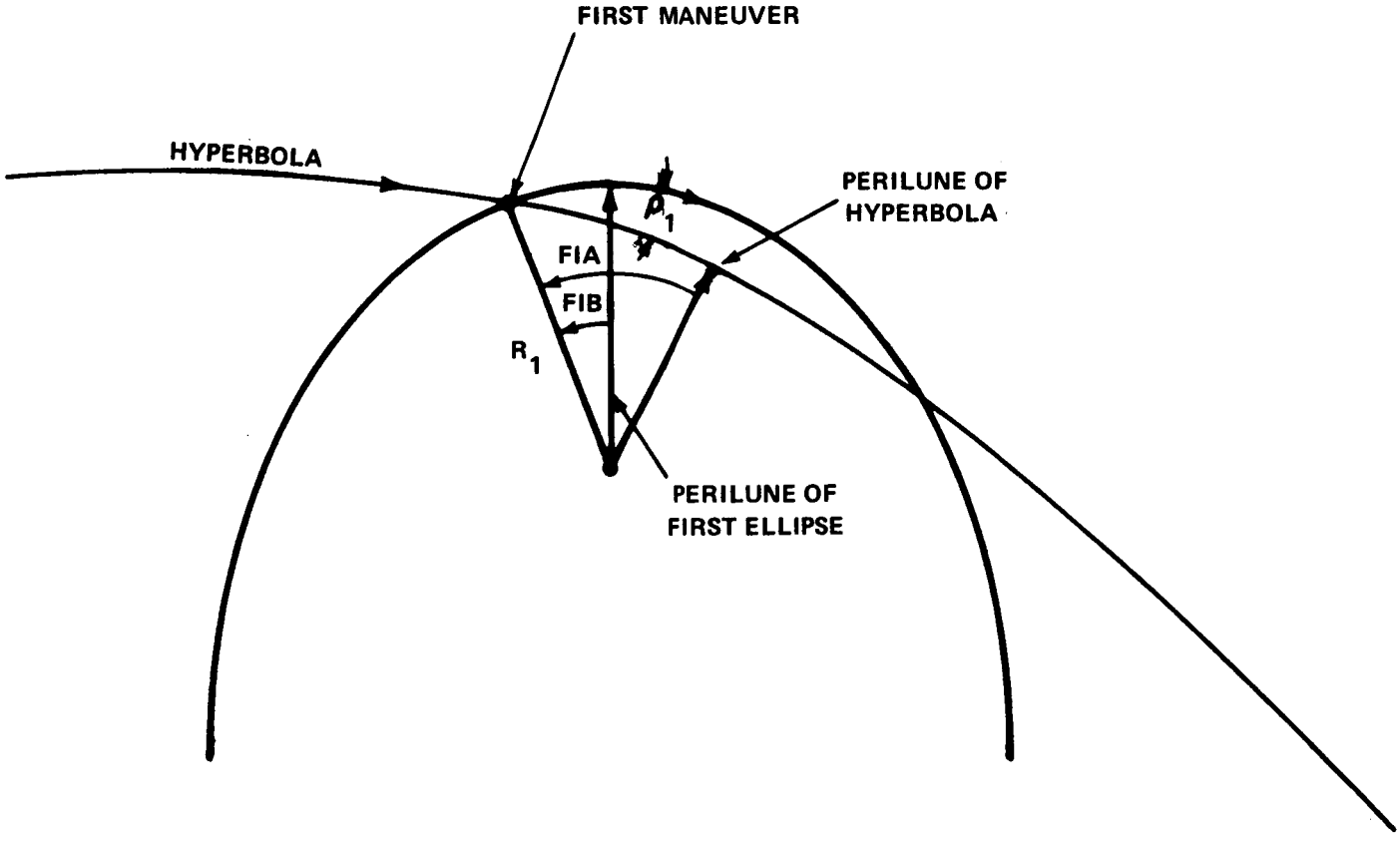

FIGURE 2 - GEOMETRY OF FIRST MANEUVER

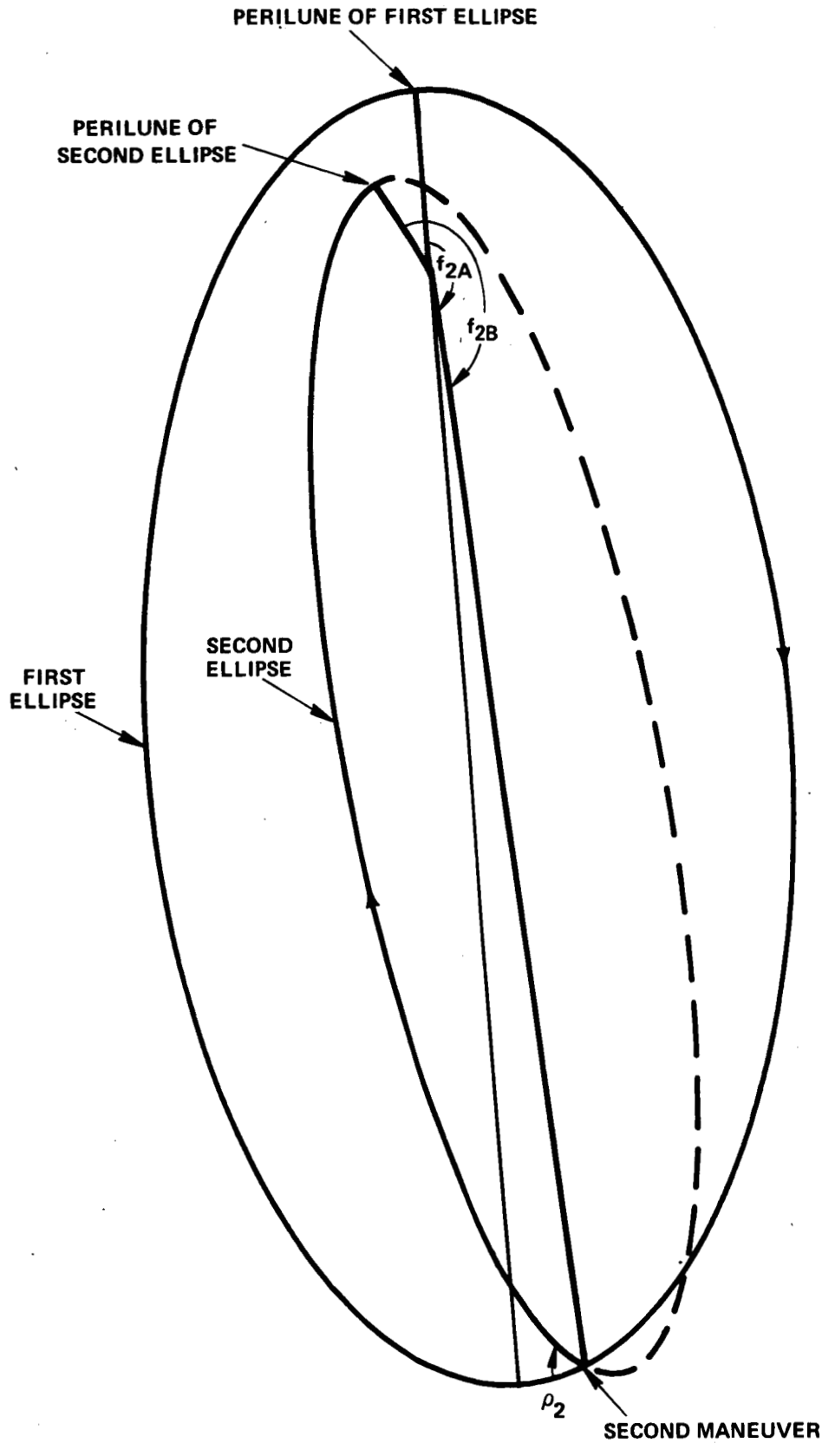

FIGURE 3 - GEOMETRY OF SECOND MANEUVER

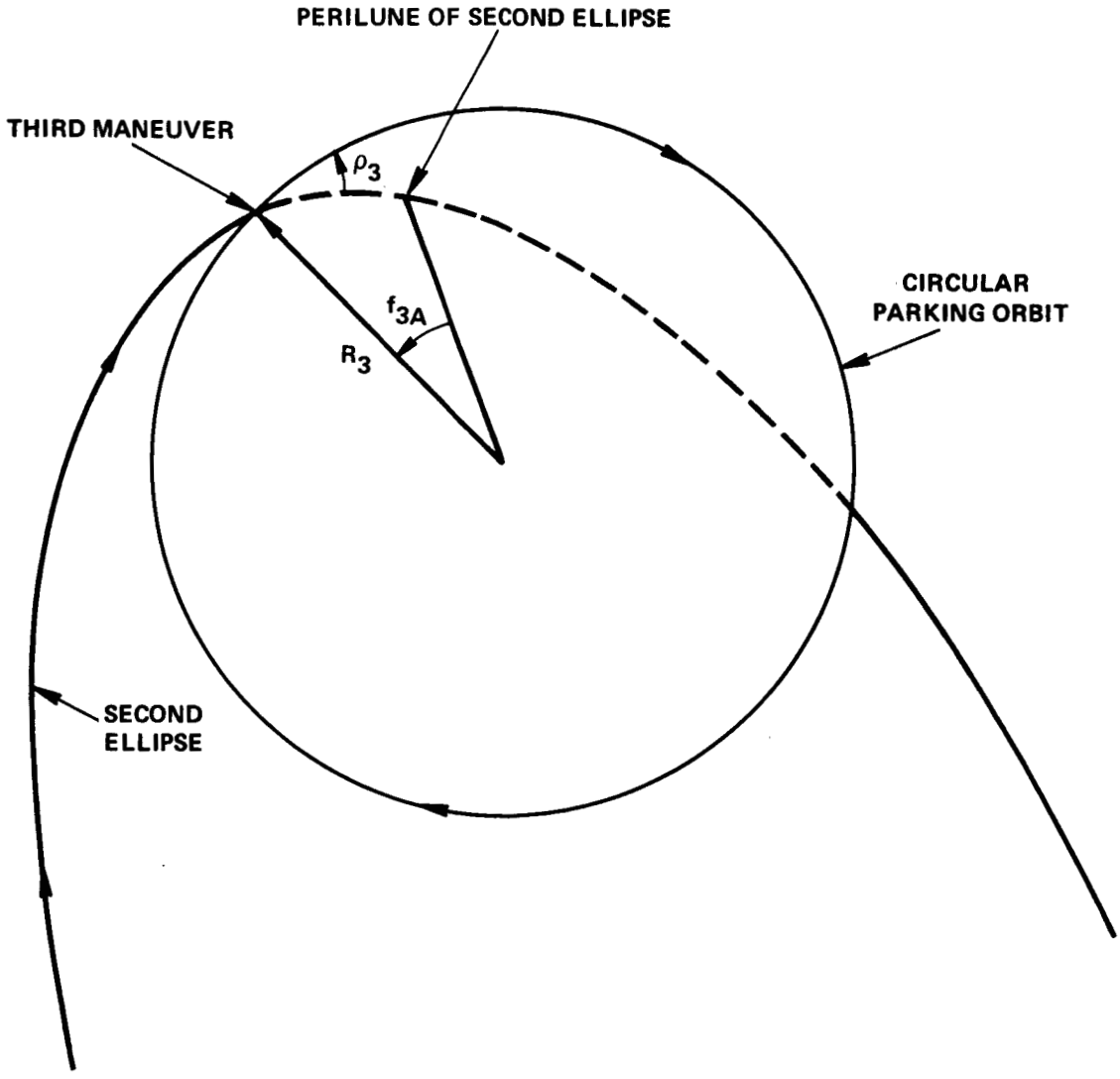

FIGURE 4 - GEOMETRY OF THIRD MANEUVER

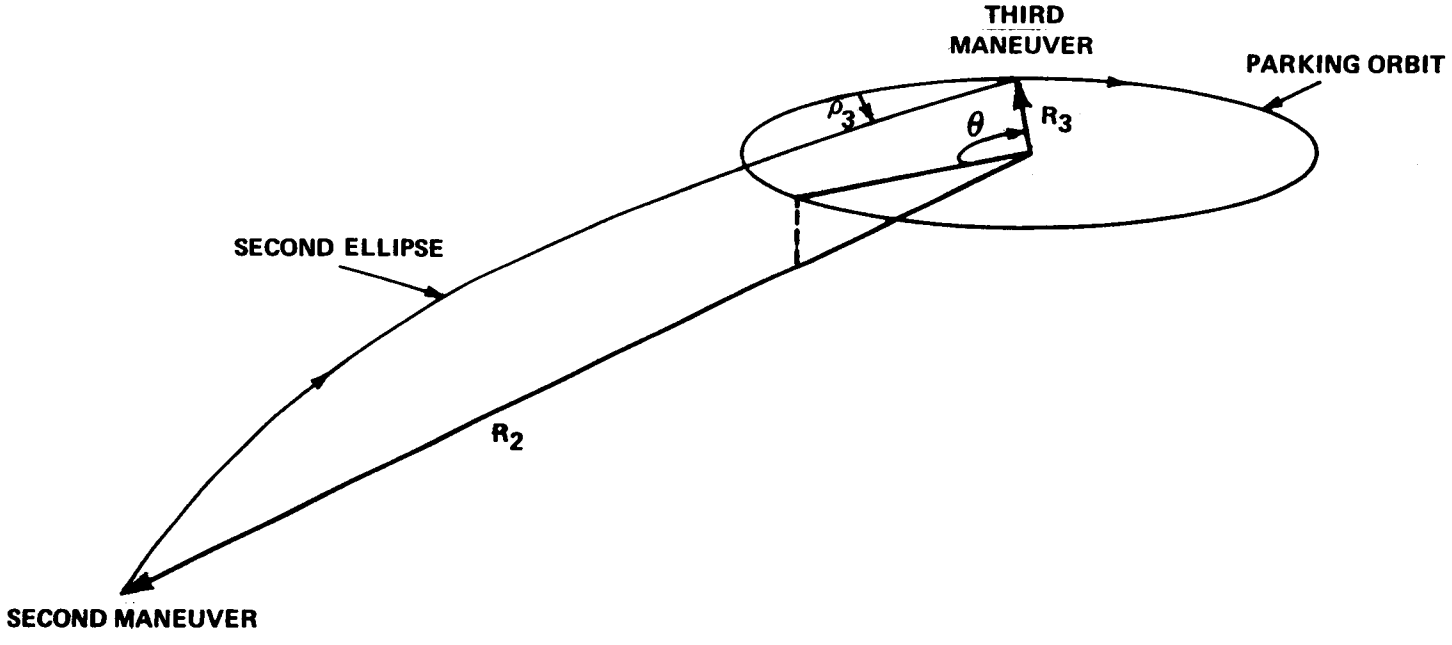

FIGURE 5 - GEOMETRY FOR OPTIMIZATION OF TRAJECTORY FROM SECOND BURN TO THIRD BURN

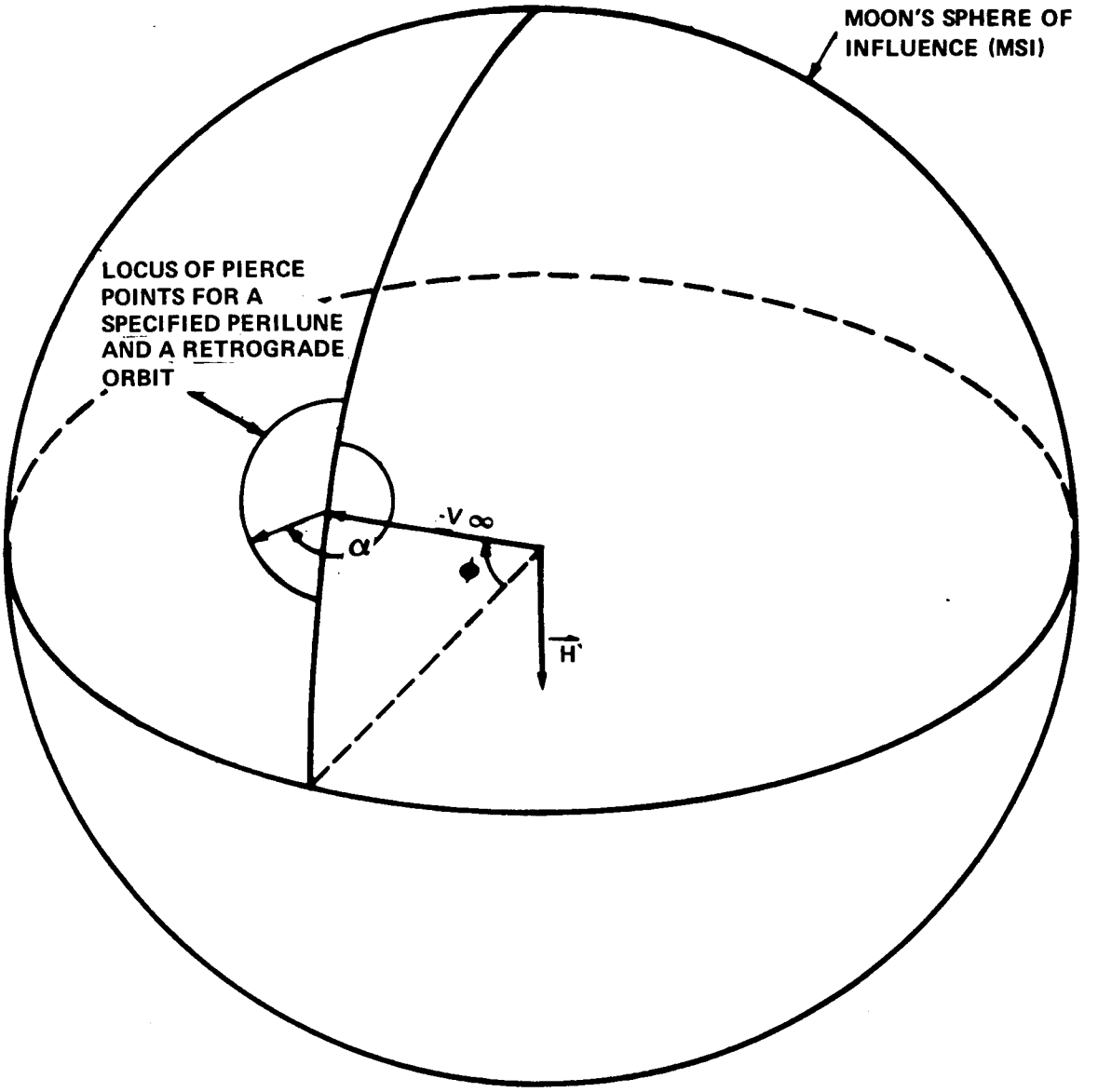

α = FLIGHT PATH AZIMUTH AT MSI

ϕ = INCLINATION OF VELOCITY VECTOR TO REFERENCE PLANE OF MSI

FIGURE 6 - GEOMETRY FOR CONSTRUCTION OF THREE-IMPULSE APPROACH HYPERBOLA AT MSI

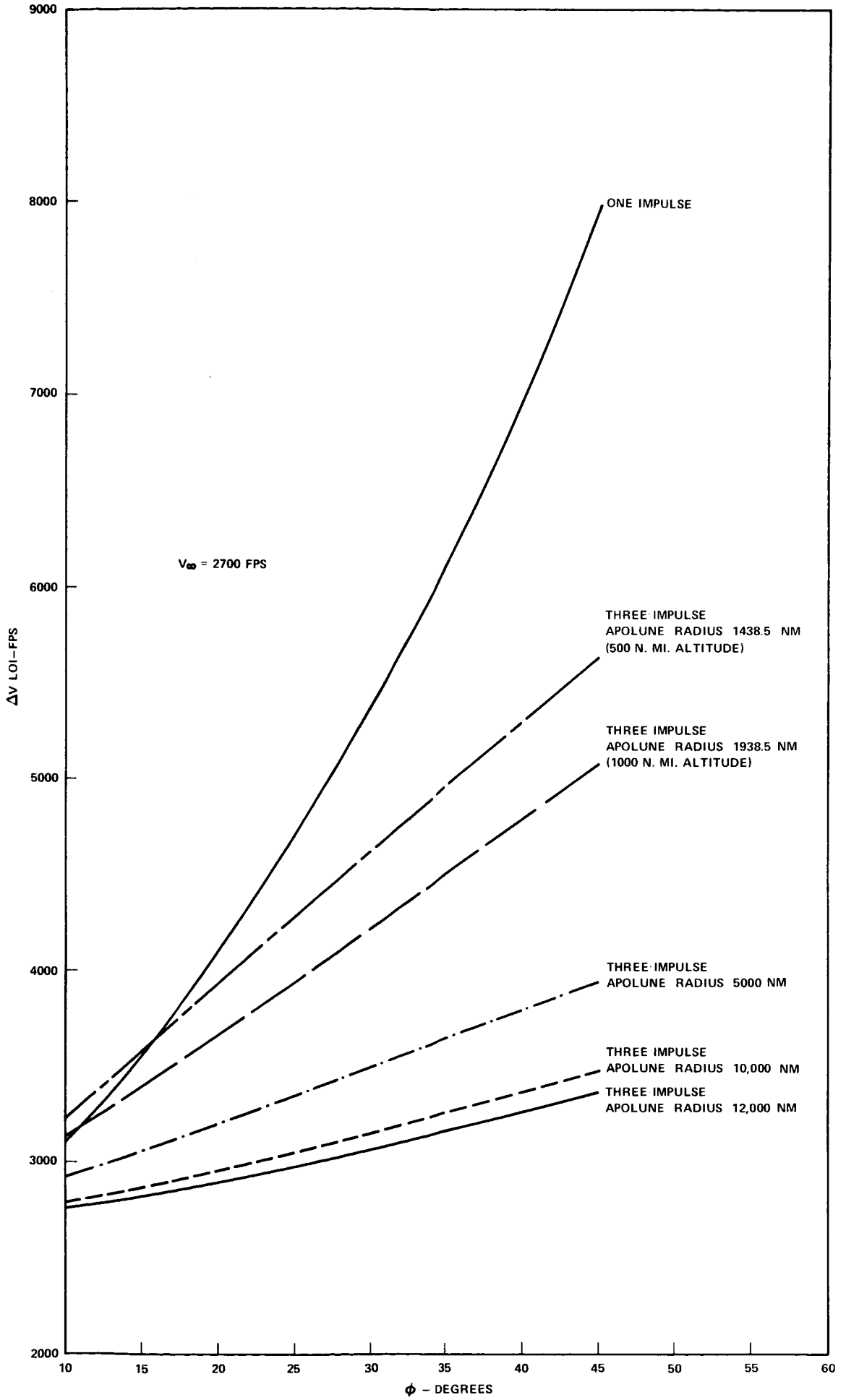

FIGURE 7–ΔV COSTS FOR ONE AND THREE IMPULSE TRANSFER VERSUS V_∞ OUT OF PLANE ANGLE

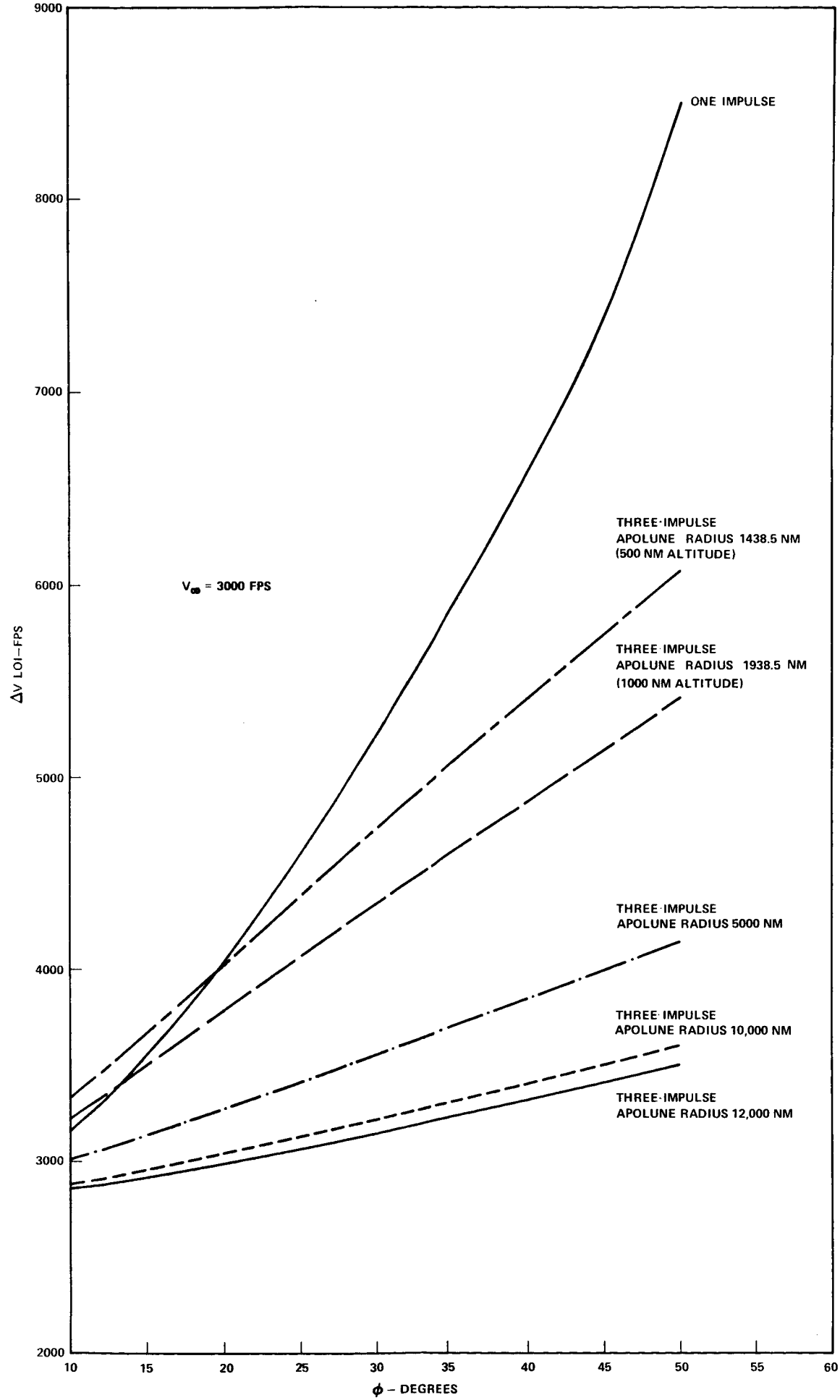

FIGURE 8–ΔV COSTS FOR ONE-AND THREE-IMPULSE TRANSFER VERSUS V_∞ OUT OF PLANE ANGLE

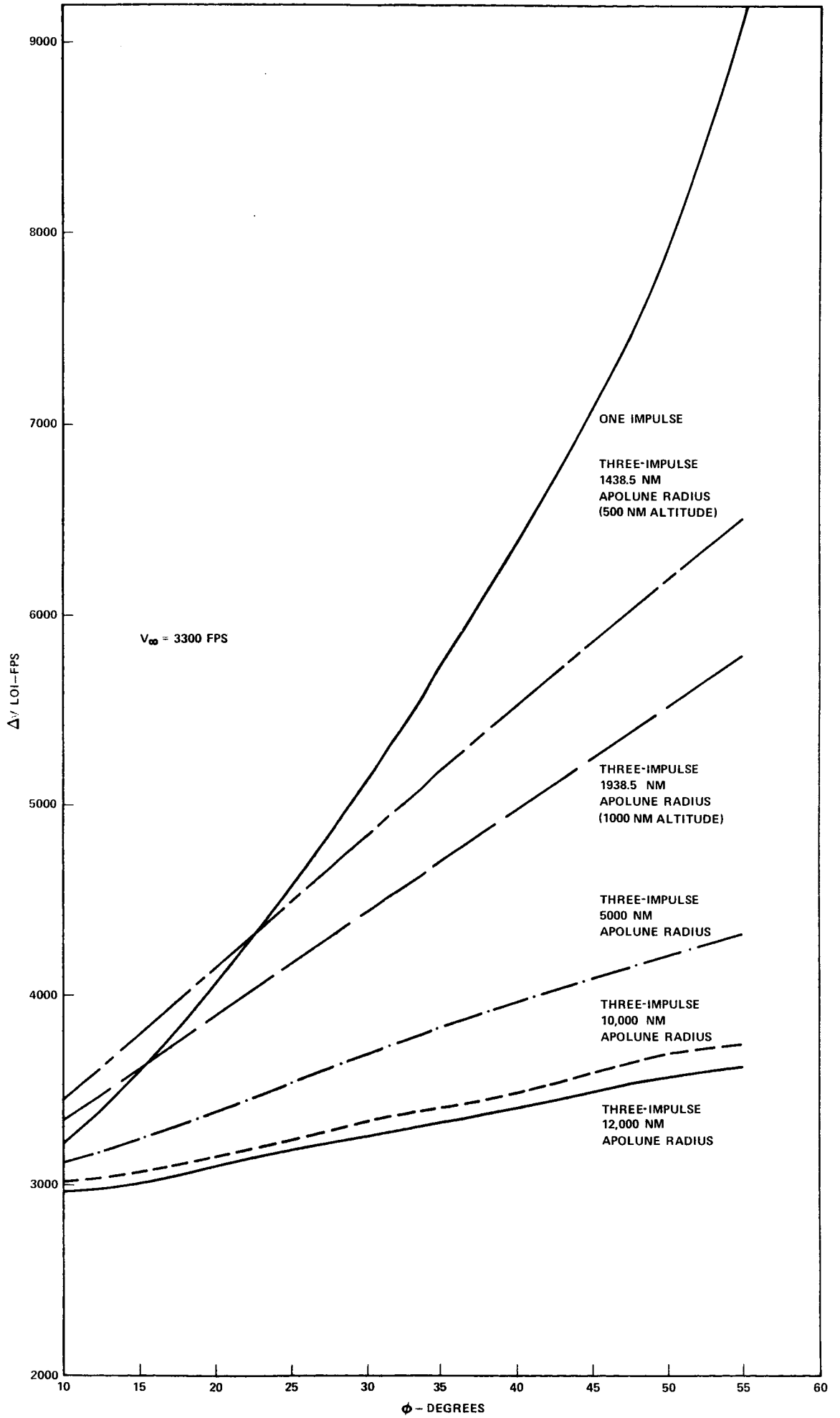

FIGURE 9–ΔV COSTS FOR ONE-AND THREE-IMPULSE TRANSFER VERSUS V_∞ OUT OF PLANE ANGLE

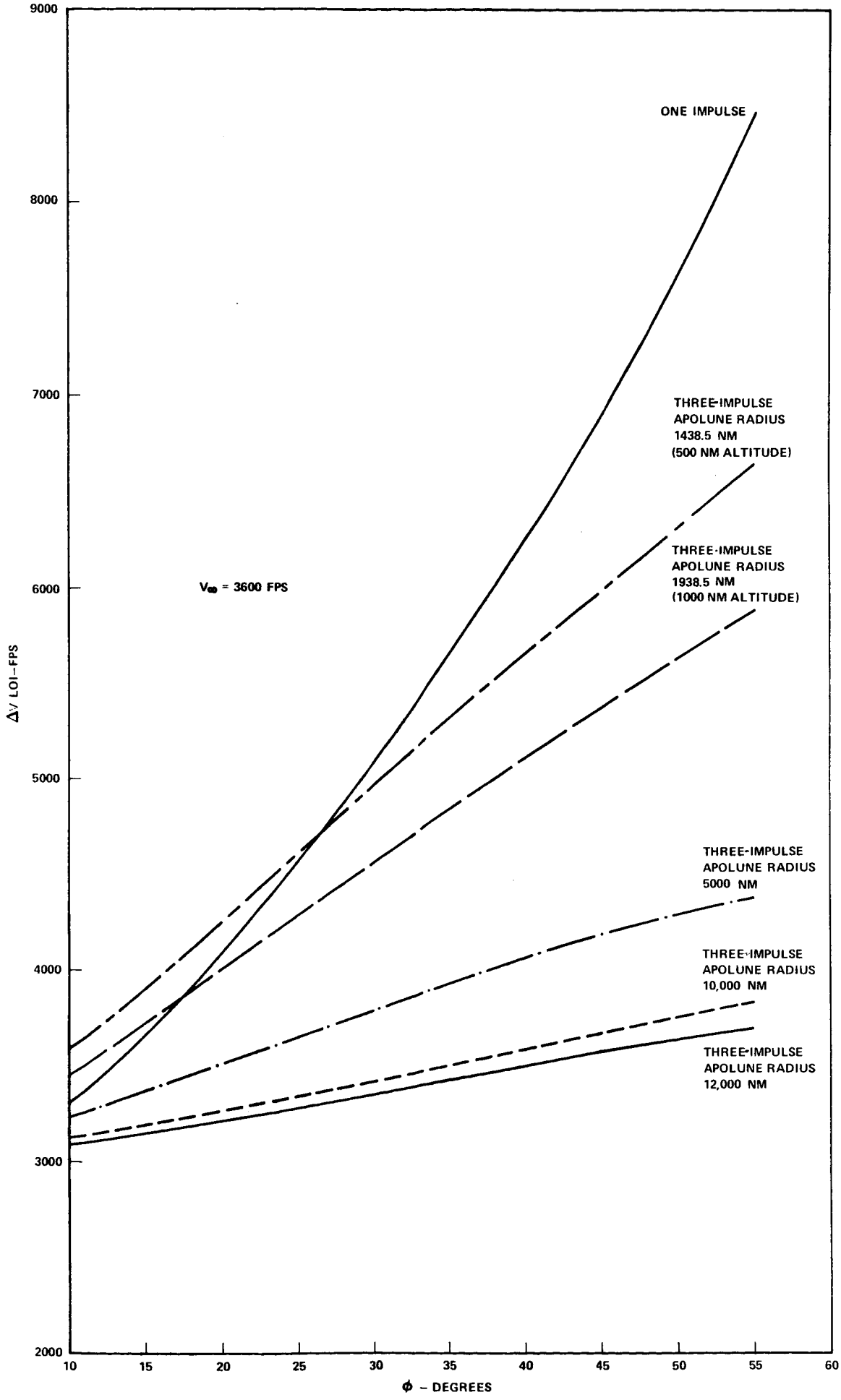

FIGURE 10–ΔV COSTS FOR ONE-AND THREE IMPULSE TRANSFER VERSUS V_∞ OUT OF PLANE ANGLE

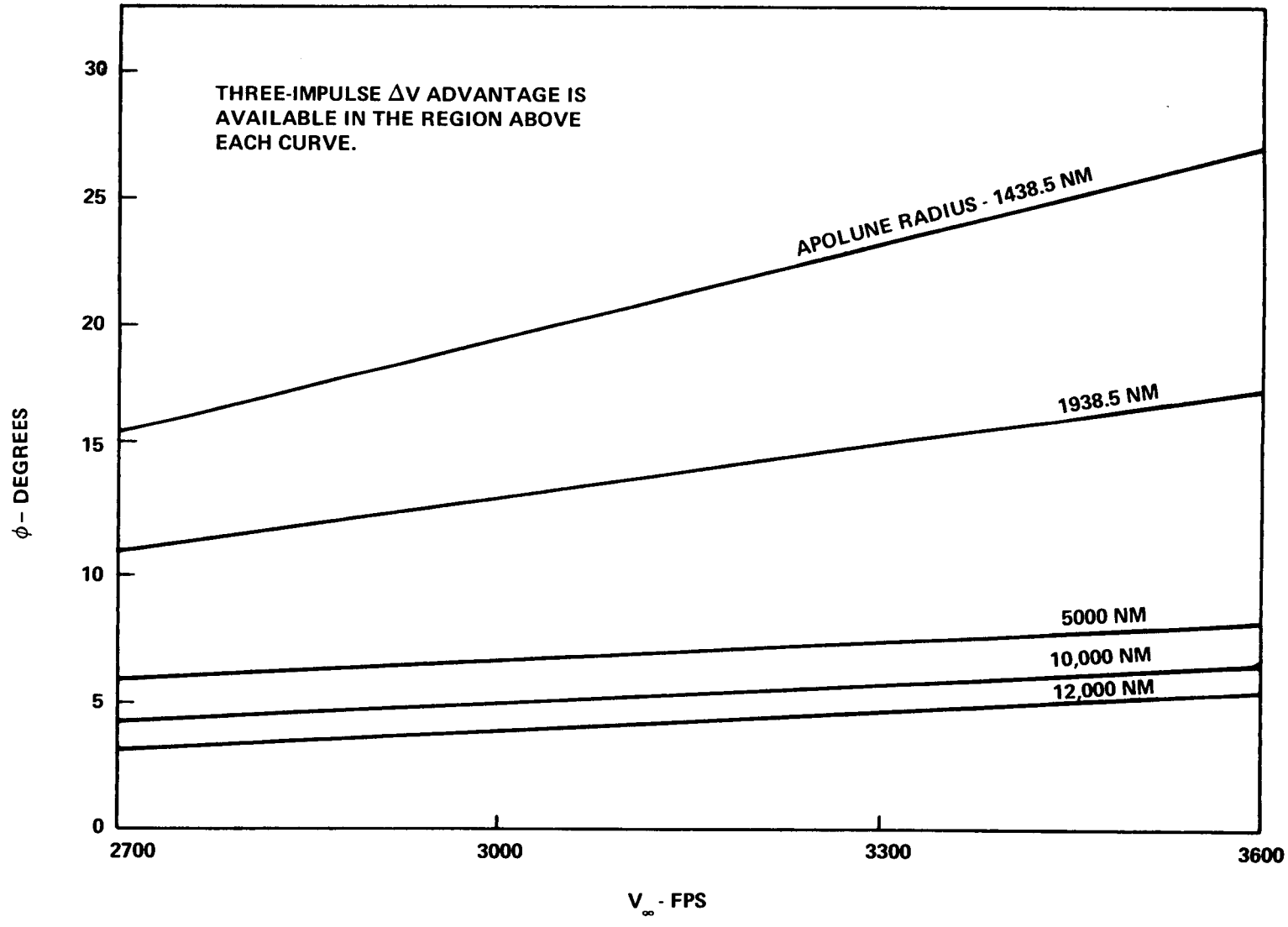

FIGURE 11 - REGIONS OF THREE- IMPULSE ΔV ADVANTAGE

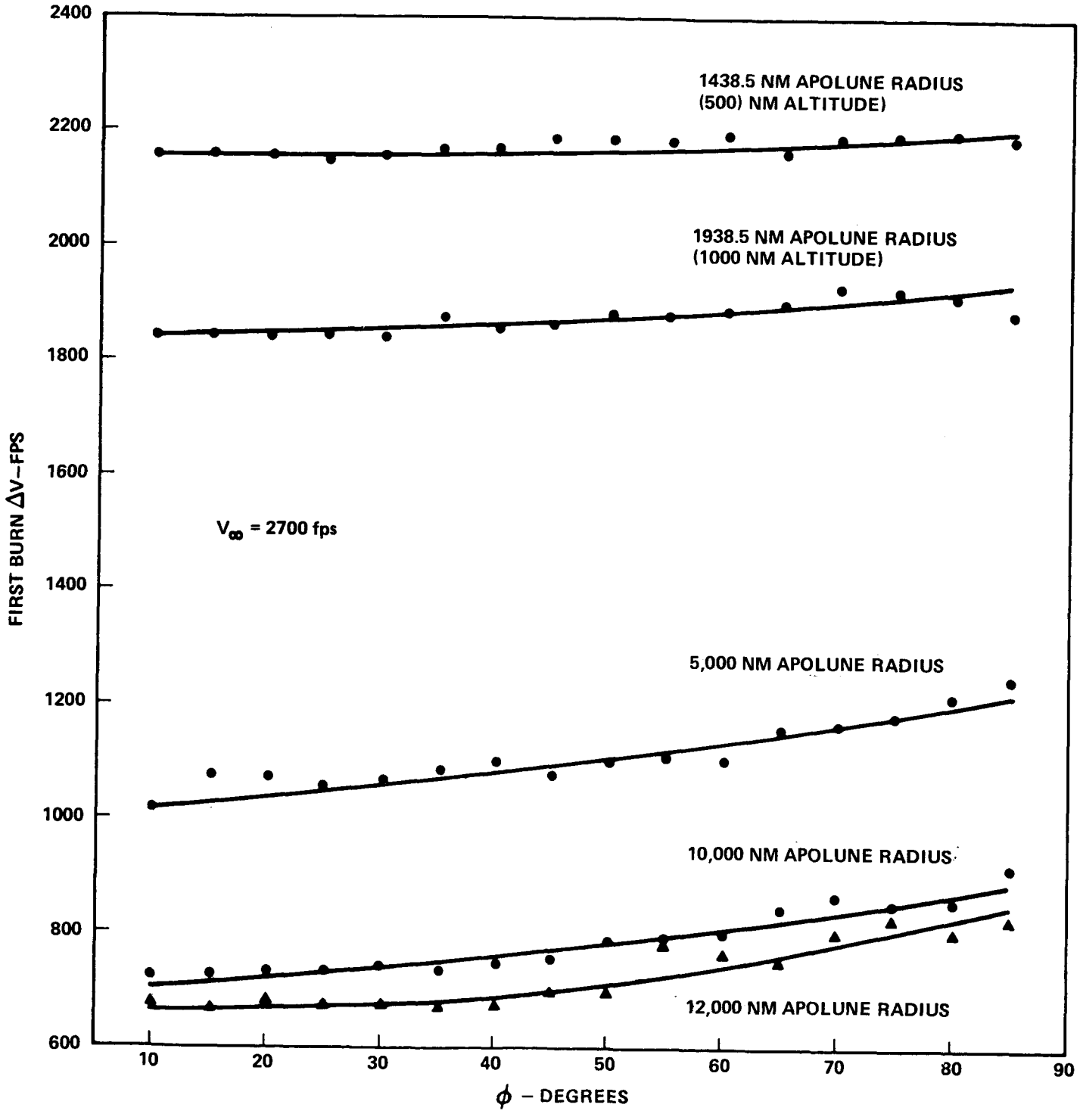

FIGURE 12–FIRST BURN ΔV COST VERSUS V_∞ OUT OF PLANE ANGLE

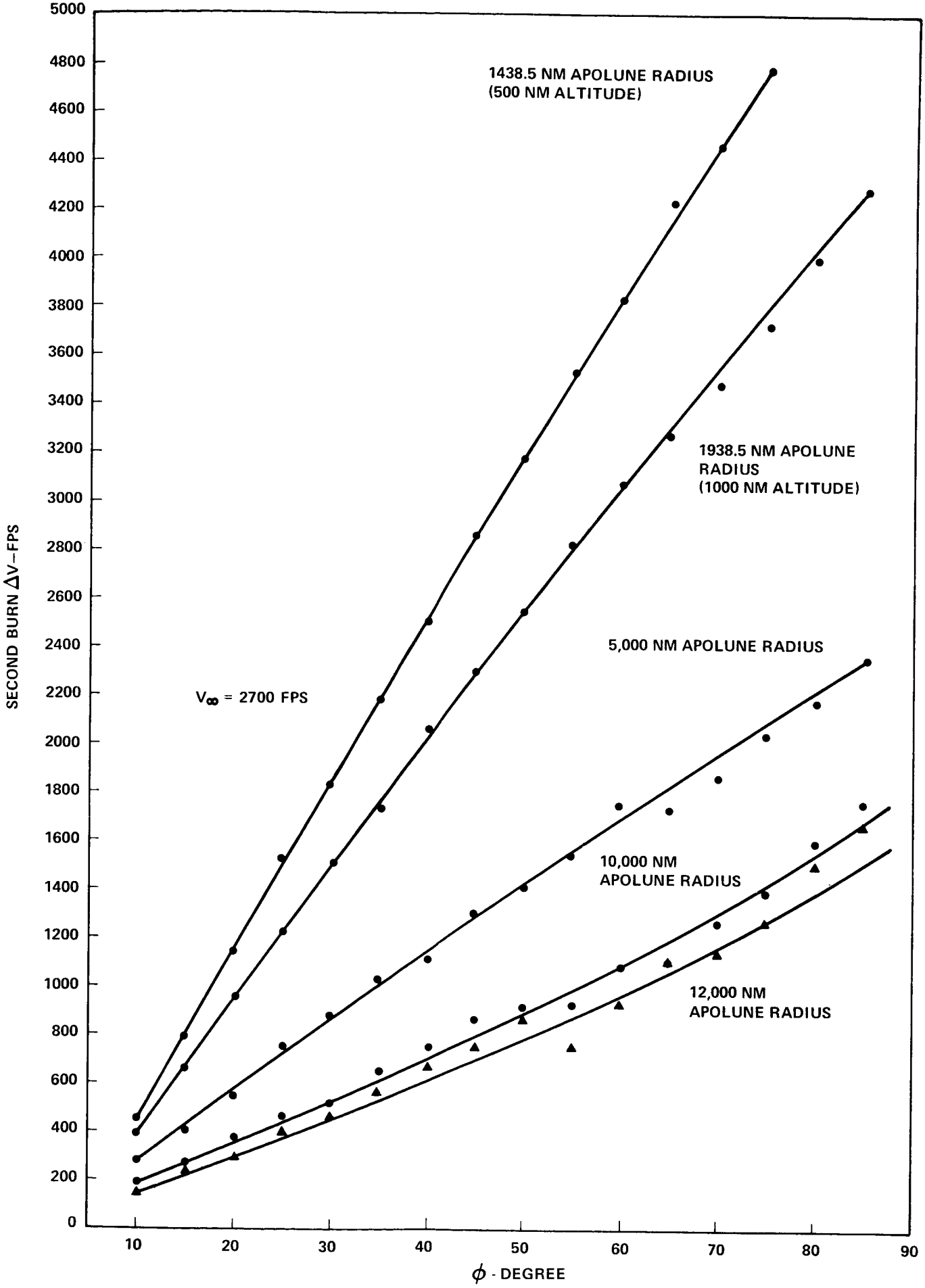

FIGURE 13–SECOND BURN ΔV COST VERSUS V_∞ OUT OF PLANE ANGLE

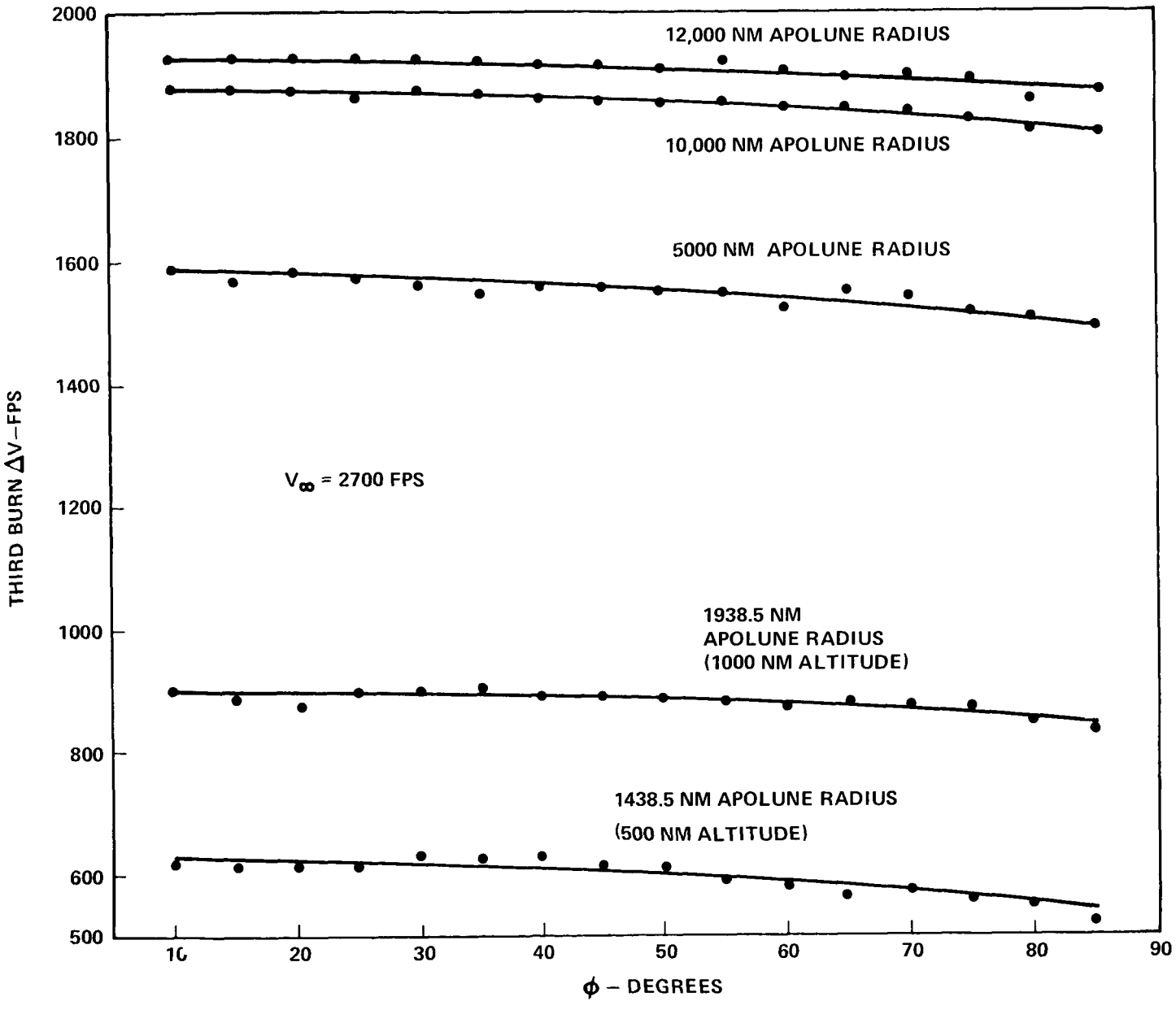

FIGURE 14–THIRD BURN ΔV COST VERSUS V_∞ OUT OF PLANE ANGLE

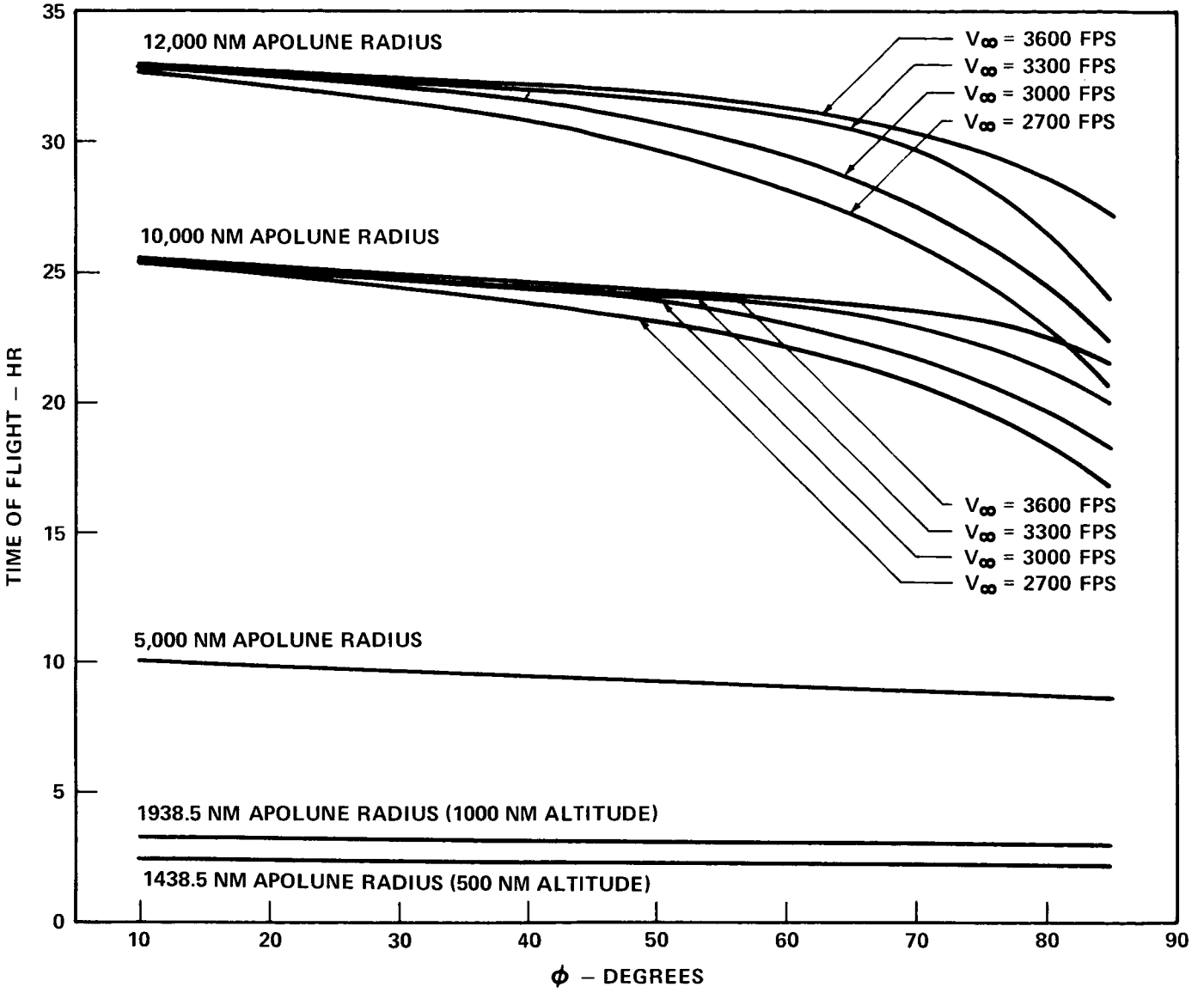

FIGURE 15–TIME OF FLIGHT FROM FIRST BURN TO THIRD BURN